Journal of Applied Fluid Mechanics, Vol. 10, No. 2, pp. 713-724, 2017.
Available online at www.jafmonline.net, ISSN 1735-3572, EISSN 1735-3645.
DOI: 10.18869/acadpub.jafm.73.239.27159

Length Scale of Free Stream Turbulence and Its Impact on Bypass Transition in a Boundary Layer

J. Grzelak[1†] and Z. Wierciński[2]

Institute of Fluid-Flow Machinery IMP PAN, Gdańsk, Poland

†*Corresponding Author Email: jj@imp.gda.pl*

(Received September 5, 2016; accepted December 13, 2016)

ABSTRACT

An experimental investigation was carried out to study the turbulent flow over a flat plate in a subsonic wind tunnel. The enhanced level of turbulence was generated by five wicker grids with square meshes, and different parameters (diameter of the grid rod $d = 0.3$ to 3 mm and the grid mesh size $M = 1$ to 30 mm). The velocity of the flow was measured by means of a 1D hot-wire probe, suitable for measurements in a boundary layer. The main aim of the investigation was to explore the influence of the free stream turbulence length scale on the onset of laminar-turbulent bypass transition in a boundary layer on a flat plate. For this purpose, several transition correlations were presented, including intensity and length scales of turbulence, both at the leading edge of a plate and at the onset of transition. The paper ends with an attempt to create a correlation, which takes into account a simultaneous impact of turbulence intensity and turbulence scale on the boundary layer transition. To assess the isotropy of turbulence, the skewness factor of the flow velocity distribution was determined. Also several longitudinal scales of turbulence were determined and compared (integral scale, dissipation scale, Taylor microscale and Kolmogorov scale) for different grids and different velocities of the mean flow $U = 4, 6, 10, 15, 20$ m/s.

Keywords: Turbulence scale; Turbulence intensity; Boundary layer; Transition; Grid; Isotropic turbulence.

NOMENCLATURE

a	acceleration parameter
C_f	skin friction coefficient
d	diameter of a grid rod
$E(k)$	turbulence energy spectrum
i	plate angle of attack
$K(u)$	flatness factor
L_S	the distance between the grid and the leading edge of a plate
L	integral length scale
Lu	dissipation length scale
M	mesh size
$R(\tau)$	time correlation coefficient
Re^{**}	momentum thickness Reynolds Number
$S(u)$	skewness factor
Tu	turbulence scale
U	velocity in x direction
$V(u)$	transverse variation
x	streamwise distance
α	slope of $Y=f(X)$ function
γ	intermittency factor
δ	boundary layer thickness
δ^*	displacement thickness
δ^{**}	momentum thickness
ε	rate of dissipation of turbulence kinetic energy
η	Kolmogorov length scale
λ	Taylor length microscale
ν	kinematic viscosity

Subscripts

l	laminar
t	turbulent; beginning of transition
θ	point, where intermittency factor γ is equal to $(e-1)/e=0.6321$
0	leading edge of a plate

1. INTRODUCTION

Traditionally, the mainstream in the study of transition of a boundary layer has been the linear stability theory, in which the unstable modes are discussed by solving the linearized fourth-order tion, for different grids, mean flow velocities and Sommerfeld equation. When the freestream turbulence (FST) level is low, the theory is very useful to predict the eigen mode in a boundary layer at the early stage of the transition, such as the Tollmien-Schlichting (TS) waves. The secondary

three-dimensional instabilities become dominant in the downstream region where the amplitude of TS waves exceeds 1% of the freestream velocity. This type of transition is commonly referred as natural transition. If the FST level is high, the initial linear growth stage is bypassed and the transition occurs early (Noro et.al. 2013). Natural transition is the dominant mode for flows, where the freestream turbulence level is less than about 1%, whereas bypass transition is the dominant mode for higher levels of freestream turbulence, which occur within gas turbine engines (Morkovin 1969).

It is possible to characterize the turbulence by its two main measures: intensity and scale, usually related to a velocity along an average stream line. The influence of turbulence intensity on transition is quite well known. The formulas describing the relation between the intensity and the onset Reynolds number are given for example by Mayle (1991), Hall and Gibbings (1972) or Abu-Ghannam and Shaw (1980). But there are still very few investigations relating to the influence of the turbulence scale on laminar–turbulent transition. Mayle (1991), in his review, suggested that the transition appears earlier when the mesh of the grid is smaller (what implies a smaller length scale). Also Jonas *et al.* (2000) suggested that the inception and the transition length depend on the turbulence scale. Their experimental results indicate that the onset of bypass transition moves downstream with decreasing length scale of turbulent disturbances at a fixed intensity of turbulent fluctuations in the leading edge plane – the laminar part of the boundary layer becomes longer. The transition region becomes shorter. Nevertheless, the transition process terminates earlier in flow with larger turbulence length scale than in flow with a smaller value of it. The turbulence intensity at the leading edge of the plate was maintained constant ($Tu = 3\%$), whilst the values of the dissipation length scale were changing: $Lu \in (2.2;33.3)$ mm. The outcome of the investigation was a following correlation:

$$\mathrm{Re}_t^{**} = (245/Lu)^{0.535} \tag{1}$$

Where $Re_t^{**}$is the momentum thickness Reynolds number $\mathrm{Re}_t^{**} = U\delta_t^{**}/\nu$ at the onset of transition, U is the mean flow velocity, δ_t^{**} is the momentum thickness at the onset of transition and ν is the kinematic viscosity of the fluid. Definitions of turbulence intensity and scales are precisely described below. Unfortunately, the above correlation is not dimensionless.

As noted in Shahinfar and Fransson (2011), in selected constant turbulence intensity at the leading edge $Tu \approx 2.6\%$, the transition occurs closer to the leading edge for increasing of the integral length scale, but for $Tu \approx 3.5\%$, the transition location moves downstream for an increase in length scale. Besides, the effect of length scale on the transition location is stronger at low level of turbulence.

In the light of the problem that still arises from the need of understanding the phenomenon of transition it seems reasonable to investigate the influence of freestream turbulence on the transition, for different conditions; different turbulence levels and scales. Despite the quite large amount of experiments designed to study the phenomenon of transition, its detailed nature is not yet fully understood.

2. REVIEW OF TURBULENCE SCALES

Barrett and Hollingsworth (2001) describe few longitudinal scales of turbulence, although the authors report there are more than ten. One can distinguish the integral scales – which are associated with the largest eddies in the flow, dissipation scales, microscales and Kolmogorov scales. The longitudinal integral scale can be defined as follows:

$$L = U\int_0^\infty \mathbf{R}(\tau)d\tau \tag{2}$$

where

$$T_E = \int_0^\infty \mathbf{R}(\tau)d\tau \tag{3}$$

is called *the Eulerian integral time scale* (Hinze 1975) and ***R(τ)*** is a time correlation coefficient:

$$R_{ii}(\tau) = \frac{\langle u_i(x,t)u_i(x,t+\tau)\rangle}{\sqrt{\langle u_i^2(x,t)\rangle\langle u_i^2(x,t+\tau)\rangle}} \tag{4}$$

The Eq. (2) is based on Taylor's hypothesis, which is valid, if the homogeneous field has a constant mean velocity and if $u/U \ll 1$ (where u-fluctuations of streamwise velocity). Another length scale (5) is related to the dissipation of turbulent kinetic energy, ε. It can be interpreted as an average dimension of eddies containing most of the energy, so-called 'energy scales' (Barrett and Hollingsworth 2001). Assuming that the turbulence is isotropic, and knowing that the dissipation of energy causes the decrease of the streamwise fluctuating component u, one can get the length scale:

$$Lu = -(u'^2)^{3/2}\Big/\left(U\frac{\partial u'^2}{\partial x}\right) \tag{5}$$

where $u' = \sqrt{\overline{u^2}}$ is the streamwise velocity standard deviation. Knowing that for the isotropic turbulence the rate of dissipation of turbulence kinetic energy, ε, can be written as:

$$\varepsilon = -\frac{3}{2}U\frac{\partial u'^2}{\partial x} \tag{6}$$

(Ames and Moffat 1990), one can determine the scale Lu as follows:

$$Lu = \frac{3}{2}\frac{u'^3}{\varepsilon} \tag{7}$$

To distinguish the length scale Lu (5) or (7) from the integral scale L (2), we will call Lu the

dissipation length scale. The measure of the average dimension of the small eddies involved in fluid motion is the time microscale of turbulence:

$$\tau_E = \left(-\frac{1}{2}\frac{\partial^2 \mathbf{R}}{\partial t}\bigg|_{t=0} \right)^{-1/2} = \left(\frac{1}{2\langle u_i^2 \rangle} \left\langle \left(\frac{\partial u_i}{\partial t} \right)^2 \right\rangle \right)^{-1/2} \tag{8}$$

which can be called the Eulerian dissipation time scale (Hinze 1975). Finally, between the time microscale τ_E and the length microscale λ, the simple relation is received:

$$\lambda = U\tau_E \tag{9}$$

The scale λ is called the Taylor microscale (otherwise, Hinze (1975) names this one the dissipation scale). The characteristic turbulence scales are also associated with the particular ranges of the turbulence energy spectrum $E(k)$. Special attention can be paid to the form of $E(k)$ in the inertial subrange, for which the Kolmogorov spectrum law is fulfilled:

$$E(k) = C_k \varepsilon^{2/3} k^{-5/3} \tag{10}$$

Where k is the longitudinal wave number and C_k is the Kolmogorov constant (for a one-dimensional spectrum). The universal equilibrium range of the energy spectrum, in which the function $E(k)$ is under the influence of only two values, i.e. dissipation ε and the kinematic viscosity of the fluid ν, can be described by the following scale:

$$\eta = \frac{1}{\mathrm{k}_\eta} = \left(\frac{\nu^3}{\varepsilon} \right)^{1/4} \tag{11}$$

This is the measure of the smallest eddies in the flow and it is called the Kolmogorov length scale (k_η is the wave number corresponding to this scale).

3. ISOTROPY OF TURBULENCE

In general, the turbulence intensity is defined as the ratio of standard deviation to the mean flow velocity, U. If the velocity field is described by the coordinate system x_i where x_1 is an axis oriented in the direction of the mean flow velocity ($U = U_1$, $U_2 = U_3 = 0$), a ratio:

$$Tu = Tu_1 = \frac{\sqrt{\overline{u_1^2}}}{U} = \frac{u_1'}{U} \tag{12}$$

Defines the longitudinal turbulence intensity, while:

$$Tu_2 = \frac{u_2'}{U} \text{ and } Tu_3 = \frac{u_3'}{U} \tag{13}$$

are components of the transverse intensity. In case of isotropic turbulence the turbulence characteristics do not depend on the spatial orientation of the coordinate system ($\overline{u_1^2} = \overline{u_2^2} = \overline{u_3^2}$).

One of the methods to assess the isotropy of turbulence is to determine the skewness factor, $S(u)$ or kurtosis (flatness factor), $K(u)$ (14), in the flow velocity distribution (Mohamed and LaRue 1990, Ting 2013).

$$S(u) = \overline{u^3} \Big/ \overline{u^2}^{3/2}, \quad K(u) = \overline{u^4} \Big/ \overline{u^2}^{4/2} \tag{14}$$

Turbulence is isotropic if $S(u) = 0$ and $K(u) = 3$, and hence, a PDF of the variable u has normal distribution. In the opinion of Batchelor (1953), the distribution can be considered as normal for the value of $K(u) = 2.86$. Jimenez (1998) gives the value of $K(u) = 2.85$. Citing Gad-el-Hak and Corrsin (1973), for a passive grid at moderate Reynolds numbers, with solidity below the unstable range, the wakes of the individual bars become turbulent close behind the grid, spread individually, and interact in some complicated way, eventually merging so that, at a large number of mesh lengths from the grid (e.g. $x/M > 30$),the turbulence is nearly isotropic.

4. EXPERIMENTAL SETUPS

The investigation was carried out in the subsonic wind tunnel of low level of turbulence, $Tu \approx 0.1$ % and with velocity range up to 100 m/s. The sketch of the test section and the details of the leading edge are shown in Fig. 1. The origin of the x-axis is defined at the leading edge of the plate. The measurement chamber with octagonal cross-section has the following dimensions (width, height, length) 600 x 460 x 1500 mm. The boundary layer was studied on the upper surface of the flat plate with the dimensions (length, width, thickness) 700 x 600 x 14 mm. The plate is fixed to the sideway windows of the chamber in two axes, 200 mm over the bottom wall, at distances of x = 150 and 600 mm from the leading edge. The first axis is immovable while the second axis can be moved up from y = 0 to 21 mm (so the leading edge moves towards negative values of the y–axis), which corresponds to the incidence angle from 0° to ⍰2.45°. The measurement chamber is equipped with three windows (250 mm long, with gaps 200 mm between) on the upper wall. The first window is located before the plate and two others are located over the plate. The probe is mounted on the removable window (which can replace one of the three windows on the upper wall of the chamber) with longitudinal slot, so it can moves in the x-direction. A micrometer screw gauge allows the movement along the y-axis.

The enhanced level of turbulence was generated by five different wicker metal grids with square meshes (Fig. 2) of the following dimensions:

1) d = 0.3 mm, M = 1 mm,

2) d = 0.6 mm, M = 3 mm,

3) d = 1.6 mm, M = 4 mm,

4) d = 3.0 mm, M = 10 mm,

5) d= 3.0mm, M = 30mm

(named appropriately G1, G2, G3, G4 and G5), where d is a diameter of the grid rod and M is a grid

mesh size. To gain different values of the turbulence intensity at the leading edge, grids were placed at different distances upstream of the plate: L_s= 450, 410, 370 and 330 mm. Also five different incoming velocities were used: U = 10, 15, 20 m/s(for G1 and G2), U = 6, 10, 15, 20 m/s(for G3), U = 6, 10 m/s(for G4) and U = 4, 6 m/s (for G5). The values of U, L_s and also dimensions of the used grids were chosen dependently whether the laminar – turbulent transition occurs in the boundary layer on the plate, for possibly the widest range of turbulence intensity and scale.

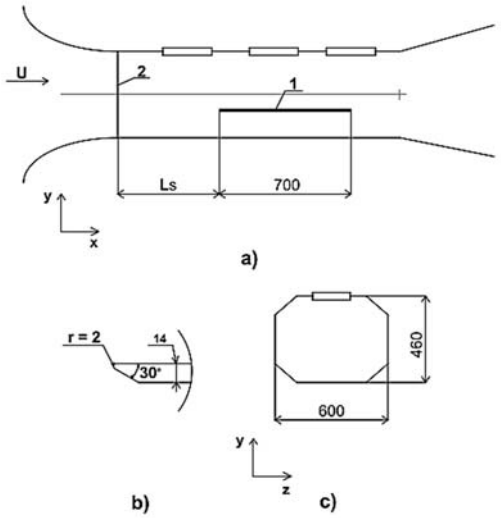

Fig. 1. Test section of wind tunnel: a) plate (1), grid (2) at the distance L_s from the leading edge, b) shape of the leading edge, c) cross-section of the measurement chamber.

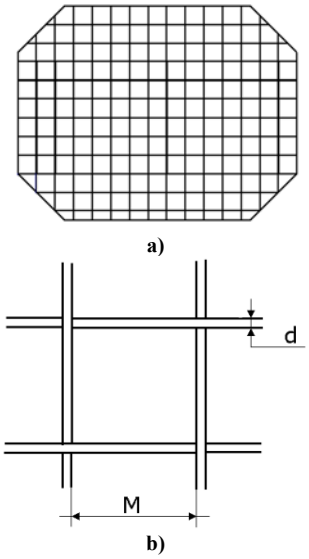

Fig. 2. Sketch of a grid (a); grid mesh (b).

The velocity and turbulence measurements were carried out by means of the Stream Line thermo anemometry system (DANTEC) with the software Stream-Ware 3.41.20 and the hot-wire probe 55P15 of DANTEC suitable for measurements in boundary layer, with diameter 5 μm, sensitive length 1.25 mm and frequency bandwidth up to 250 kHz The sampling frequency of the velocity signal in the present experiment was f = 6 kHz; 40000 samples were taken, i.e. for about 6.67 s. The example of the turbulence energy spectrum of velocity fluctuations u above the boundary layer, for grid G3, mean streamwise velocity U = 10 m/s, L_S = 450 mm and the distance from the leading edge x = 230 mm, is shown in Fig. 3. The solid line represents the Kolmogorov's law (10) and determines the inertial subrange of the energy spectrum.

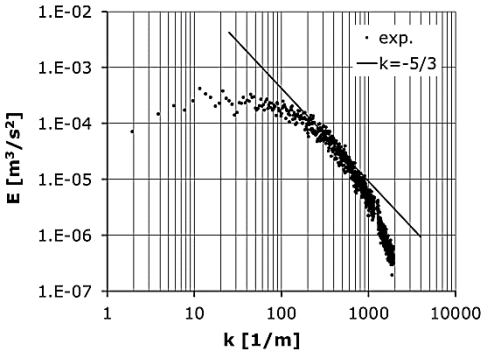

Fig. 3. Turbulence kinetic energy spectrum.

Before the every series of measurements the calibration of system was carried out. Resulting streamwise uncertainties in U were about ± 1 %. The example of calibration curve, for G3 and U = 10 m/s, together with error bars, is presented in Fig. 4. The velocity ranges from U = 0.7 to 12.5 m/s; E [V] denotes the voltage drop on the probe wire.

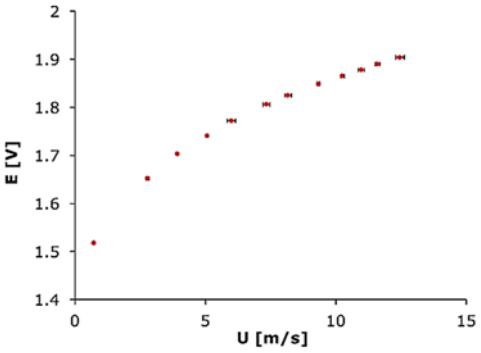

Fig. 4. The calibration curve.

5. INVESTIGATION RESULTS

5.1 Turbulence Intensity Behind Grids

Study investigated the effect of the free stream turbulence length scale on the transition point. To get the values of turbulence intensity and turbulence scale along the test section the measurements of mean streamwise velocities and velocity fluctuations behind all grids were carried out first. The

measurements were done before and over the flat plate (the probe was set at least 50 mm over the plate surface where there is no plate effect). Distance between the subsequent measuring points was 30 mm. Fig. 5 displays the decay power law, $Tu = c(x/d)^{-n}$, given by Roach (1986), for grids G1 – G5. In accordance with the Roach's experiments, a value of the experimental factor c is equal to 0.8 and n = 5/7 (the solid line in Fig. x). Baines and Peterson (1951) give the values: c = 1.12, n = 5/7 (the dashed line). The turbulence intensity of the flow was determined from the Eq. (12).

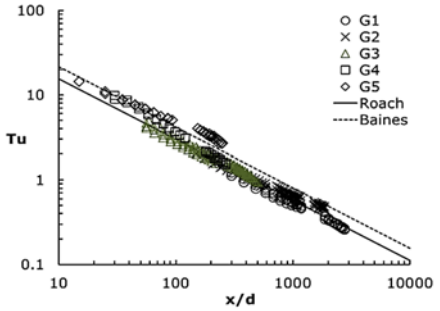

Fig. 5. The decay power law.

5.2 Isotropy and Homogeneity of Turbulence

Many of the formulas listed in this article refer to the isotropic and homogeneous turbulence, so it was important to assess what kind of turbulence we have to do with in the experiment. First of all, isotropy of turbulence of the flow behind the grids was investigated. For reference case, skewness factor along the test section of the tunnel in case without the turbulence generator (grid) and without the flat plate was measured. The first measuring point position was 100 mm from the measurement chamber inlet (230 mm from the upper wall, i.e. in the middle of the chamber). Values of skewness for mean flow velocities U = 6, 10, 15 m/s are displayed in Fig. 6. The turbulence intensity Tu didn't exceed, in this case, the value of 0.13 %. As one can see, $S(u)$ for all three flow velocities ranges approximately from 0 to 0.06 throughout the measured region.

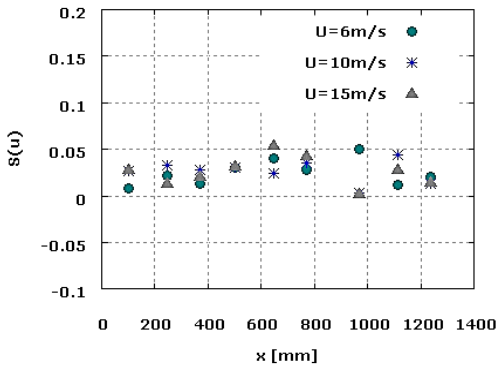

Fig. 6. Skewness along the measurement chamber in case of no turbulence generator, for mean flow velocities U = 6, 10 and 15 m/s.

According to the previous investigations (Grzelak, Wiercinski, 2015), turbulence of the flow behind grids was considered to be nearly isotropic from the distance $x/M \approx 60$. The values of x/M, $S(u)$, $K(u)$ for grids G1 – G4 and for all flow velocities used in the experiment are displayed in Table 1. (For G1 the distance is $x/M = 90$, but it was the first point measured behind the grid, i.e. x = 90 mm).

Table 1 Values of the distance x/M for grids G1 – G4, from which turbulence is considered to be isotropic

Grid	U[m/s]	S(u)	K(u)	X/M
G1	10	0.050	3.00	90
	15	0.057	3.00	90
	20	-0.033	3.03	90
G2	10	0.036	2.90	60
	15	0.036	2.90	60
	20	0.057	2.88	70
G3	6	0.049	2.93	60
	10	0.059	2.94	66
	15	0.028	2.94	56
	20	-0.024	2.97	66
G4	6	0.047	2.91	61
	10	0.060	2.94	67

The homogeneity of turbulence behind all grids used in the experiment was investigated. As a method to investigate the homogeneity of the flow behind the grid, one can use *transverse variation* of the difference of the root mean square of the downstream velocity, $\overline{u^2}^{1/2}$, and the centreline value normalized by the centreline value, $\overline{u_0^2}^{1/2}$ (Mohamed and LaRue 1990):

$$V(u) = \frac{\overline{u^2}^{1/2} - \overline{u_0^2}^{1/2}}{\overline{u_0^2}^{1/2}} \tag{15}$$

In the opinion of Gad-el-Hak and Corrsin (1973) homogeneous turbulence, $V(u) \approx 0$, can be obtained for $x/M > 30$, while Valente and Vassilicos (2011) claim that for regular grids the turbulent flow should be considered as homogeneous in transverse planes even for $x/M > 25$. Mohamed and LaRue (1990) obtained, for example, $V(u) = 0.03$ and $S(u) \approx -0.03$ to 0.03 from $x/M > 40$, what provides ones means, in their opinion, to assess the approach of the flow to an isotropic and homogeneous conditions. In present investigation, for grids G1 – G4, $V(u)$ did not exceed the value of 0.07 in all measured area, oscillating around zero over the plate ($V(u) \leq 0.03$), so we can assume that turbulence is approaching to homogeneous conditions for these grids. In case of G5 variation was still too high; $V(u) \approx 0.2$ over the whole plate (the exact investigation results related to the transverse variation calculations one can find in the paper of Grzelak and Wiercinski (2015)).

Finally, it can be stated that turbulence of the flow over the plate is nearly isotropic and homogeneous for grids G1 – G4 (grid G5 produced anisotropic, inhomogeneous flow, which was due to the fact that the mesh of G5 was too large to allow the exploration of regions with sufficiently large values of x/M where homogeneity could be expected to be recovered).

5.3 Scales of Turbulence

To investigate the turbulence scale dependence on the transition inception, which was the main goal of the experiment, determining the length scale behind the grid was first needed. To determine the dissipation scale Lu and Kolmogorov scale η, knowledge of the rate of turbulence kinetic energy dissipation ε was required. Therefore the turbulence energy spectrum $E(k)$ was determined by means of Fourier transform in Matlab.

In Fig. 9 different kinds of turbulence length scales are presented, for the selected grid G3, the velocity of the flow U = 10 m/s and the grid distance L_S= 450 mm from the leading edge of the plate. The integral scale L, associated with the largest eddies in the flow has of course the largest dimension, next we have a bit smaller dissipation scale Lu, Taylor microscale λ and finally the Kolmogorov scale η as the measure of the smallest eddies. The results of Jonas (2000), for dissipation scale Lu, was provided for comparison. The solid line in Fig. 9 corresponds to the typical variation of the integral scale (see Laws and Livesey 1978):

$$L = A_L\left((x - x_0)/M\right)^{1/2},\ M/d \sim 5 \tag{16}$$

Where A_L= 2 or A_L= 0.1 (Kurian and Fransson 2009); x_0 is a virtual origin of turbulence. For the present grid G3: M/d = 2.5 and x_0 = 8.7 mm. The dashed line in Fig. 7 corresponds to the variation of the Taylor microscale given by Hinze (1975):

$$\lambda = \left(20\nu(x - x_0)/U\right)^{1/2} \tag{17}$$

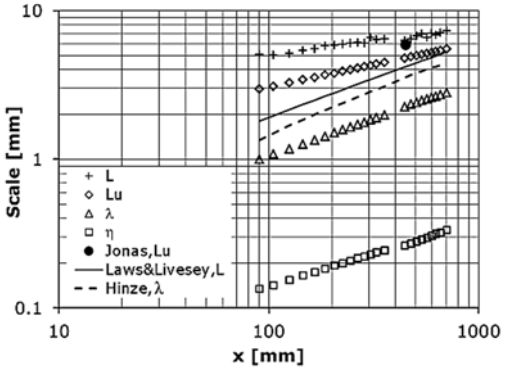

Fig. 7. Scales of turbulence behind the grid G3, for U = 10 m/s; + L – integral scale (2), ◊ Lu – dissipation scale (7), Δλ – Taylor microscale (9), □ η – Kolmogorov scale (11).

5.4 Velocity Profiles in the Boundary Layer

Next, the velocity profiles in the boundary layer on a flat plate were measured. Distance between the measuring points in the x direction was 20 mm. The origin of the x-axis was the leading edge. In each of the points the boundary layer profile was measured. Each profile consisted of about 40 points; the first one at 25 mm and the last one about 0.1 mm above the plate surface. The distance from the hot-wire to the plate, Y_0, was measured by means of the method called 'hydraulic zero' (Epik 1998). If the wire was very close to the surface, thermo anemometric response was like velocity started to increase. Then the measurements were stopped. For the further procedure it was assumed that the last measured point was Y = 0 mm from the wall. To find a real Y_0, the velocity profile $U = f(Y)$ was examined (Fig. 8). Because $U|_{wall}$= 0, a tangent to the profile, $U = (\mathrm{d}U/\mathrm{d}Y)Y+B$, was conducted through the last few points of the profile (points for which the velocity seemed to increase, were rejected). The intersection of the tangent and the abscissa gives, as the absolute value $|Y_0|$, the searched distance from the hot-wire to the plate surface.

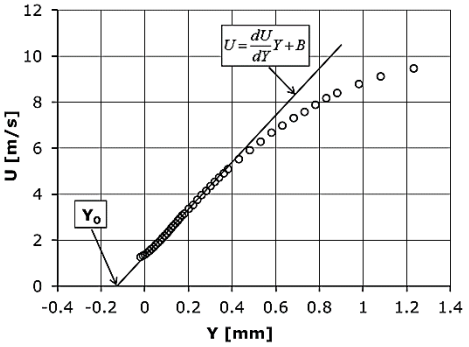

Fig. 8. Velocity profile in a boundary layer, for G3, U = 10 m/s, L_S = 450 mm.

The measured boundary layer thickness, defined as $U(\delta) = 0.99\,U_\infty$, was from about 1.3 to 3 mm for laminar boundary layer and from about 9 to 14 mm for turbulent boundary layer. The examples of the boundary profiles, for grid G3, U = 10 m/s, L_S = 450 mm, are presented in Figs. 9 and 10, in comparison with other well-known profiles: the Blasius profile for laminar boundary layer (Fig. 9) and the law of the wall for turbulent boundary layer (Fig. 10). In both cases, three different distances, x, from the leading edge are taking into account. First one is x = 110 mm, where the boundary layer is still laminar (shape factor $H = \delta^*/\delta^{**} = 2.25$). Next profile, for x = 370 mm, lays in the transition region (H=1.91; the onset of transition is estimated to x_t = 313 mm). The last profile, x = 650 mm, corresponds to the turbulent boundary layer (H = 1.42).

To avoid separation at the leading edge the incidence angle of the plate i = –1.63° was set (boundary layer with favourable pressure gradient). Therefore a velocity gradient along the plate was measured. A value of the acceleration parameter:

$$a = \frac{\nu}{U^2}\frac{dU}{dx} \tag{18}$$

Where U is the mean flow velocity and v is the

kinematic viscosity, was approximately equal to $a \approx 2.7 \cdot 10^{-7}$. This showed that compared with the critical acceleration parameter needed to accomplish *relaminarization*in boundary layers ($a_{crit} \sim 3.5 \times 10^{-6}$, see e.g. Sreenivasan1982), the applied pressure gradient is quite moderate. In terms of velocity increase it is from about 2 to 4%.The effect of favourable pressure gradient on boundary layer receptivity and on turbulence characteristics one can find e.g. in Xu *et al.* (2016), Johnson and Pinarbasi (2014), Kurian and Fransson (2009). According to the experiment of the last authors, who reached the acceleration parameter maximally equal to $2.5 \cdot 10^{-7}$, an important result is the observed reduction in turbulence length scales (20-30%) for large mesh widths (M = 36 mm), which was absent for small mesh widths (M = 4.2 mm).

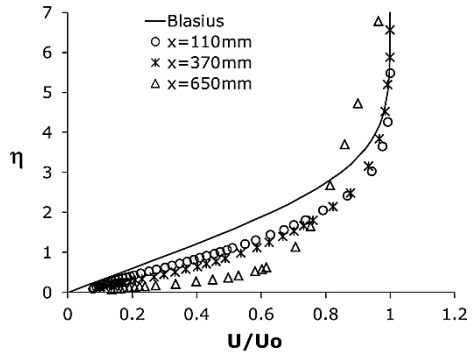

Fig. 9. Blasius profile for the laminar boundary layer; boundary profiles for G3, U = 10 m/s and three distances x from the leading edge.

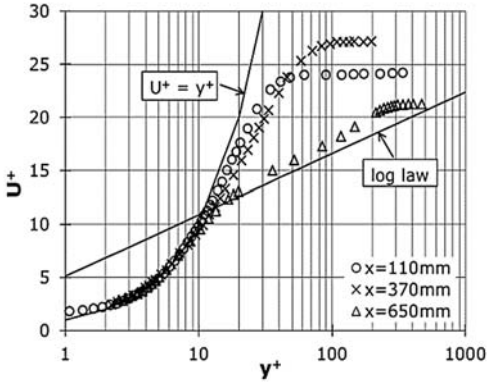

Fig. 10. The law of the wall for turbulent boundary layer; boundary profiles for G3, U = 10 m/s and three distances x from the leading edge.

5.5 Method of Determining the Transition Inception

Having determined the length scale of turbulence, the momentum thickness Reynolds number of the onset of the transition, Re_t^{**}, needs to be calculated, to find the correlation function. The values of the local skin friction coefficient, C_f, were used to observe the region of transition and to determine the intermittency factor by means of Eq. (19), derived from the model of Dhawan and Narasimha (1958).

$$\gamma = \frac{C_f - C_{fl}}{C_{ft} - C_{fl}} \tag{19}$$

C_{fl} and C_{ft} are local skin friction coefficients in laminar and turbulent regions of the flow, respectively. They were determined by means of the Blasius solution for the laminar and turbulent boundary layer (Blasius 1913): $C_{fl}=0.664(\mathrm{Re}_x)^{-0.5}$, $C_{ft}=0.0595(\mathrm{Re}_x)^{-0.2}$. The intermittency factor was first defined by Townsend (1948) as the fractional time spent by a fixed probe in the turbulent fluid. Next, another formula for intermittency factor, γ (20), was used to set the characteristics of the laminar-turbulent transition. To describe γ in the transition region the cumulative distribution function of three-parametric Weibull probability distribution was used (Dhawan and Narasimha 1958, Emmons 1951):

$$\gamma = 1 - \exp\left(-\frac{\mathrm{Re}_\theta^{**} - \mathrm{Re}_t^{**}}{\mathrm{Re}_\theta^{**} - \mathrm{Re}_t^{**}} \right)^{\alpha} \tag{20}$$

The description of the Weibull distribution and its application in different engineering fields can be found in Lipson and Sheth (1973) or Wadsworth (1989). In the Eq. (20) α is the shape parameter, Re_t^{**} – the point where transition begins, Re_θ^{**} – (characteristic length) the point where intermittency factor is equal to (e − 1)/e = 0.632, where e is a base of the natural logarithm. Taking twice the logarithm of Eq. (20) and substituting Eq. (19) for γ,it is possible to determine the Re_t^{**} obtaining the linear relationship (Lipson and Sheth 1973):

$$Y = \alpha X + C \tag{21}$$

where:

$$X = \ln\left(\frac{\mathrm{Re}_\theta^{**} - \mathrm{Re}_t^{**}}{\mathrm{Re}_\theta^{**} - \mathrm{Re}_t^{**}} \right)$$

$$Y = \ln\ln\left(\frac{1}{1 - \left(C_f - C_{fl}\right)/\left(C_{ft} - C_{fl}\right)} \right) \tag{22}$$

$$C = -\alpha \ln\left(\mathrm{Re}_\theta^{**} - \mathrm{Re}_t^{**} \right)$$

A shape parameter α is a slope of the function $Y = \alpha X + C$. This method was validated for the experimental data presented in the paper of Wiercinki (1997).

The value of Re_t^{**} was initially estimated from Fig. 11, which displays γ, determined from the Eq. (19), in the function of Re^{**}. The presented case relates to the grid G2, U = 15 m/s and L_S = 330 mm. Re_θ^{**} (marked as Δ in Fig. x) was estimated by means of the linear regression made of two points surrounding the value of γ = 0.632. Next, the guessed values of Re_t^{**} were tested. A graph of the function (21) for four different exemplary values of Re_t^{**} = 235, 248, 261, 274 is presented in Fig. 5. It is apparent from the picture that the best linearity of the relationship (21) was reached for Re_t^{**} = 248, so this value was estimated as the beginning of the transition.

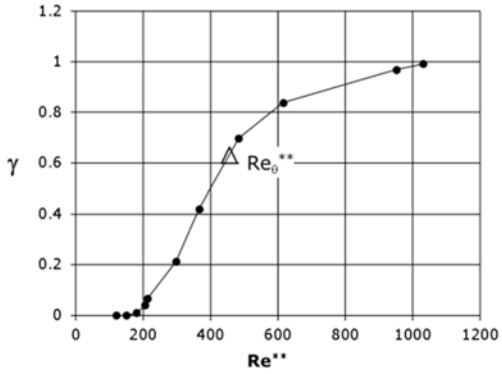

Fig. 11. Intermittency factor, determined from the Eq. (19), in the function of Re^{**}.

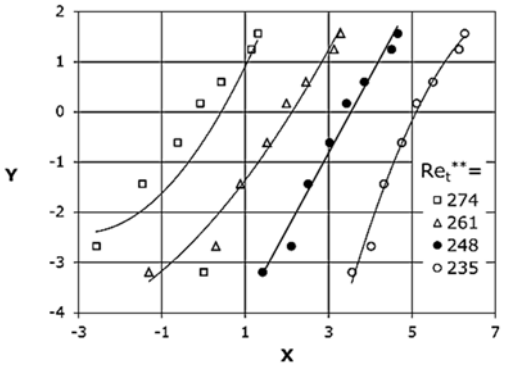

Fig. 12. Function (21).

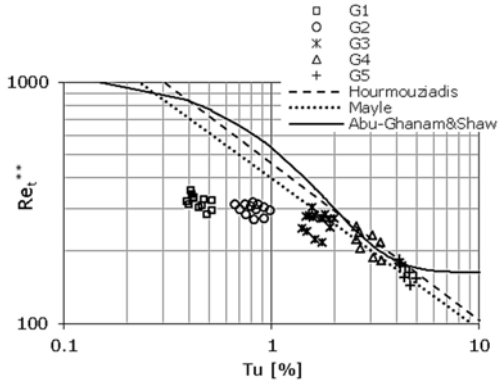

Fig. 13. Momentum thickness Reynolds number at the onset of transition as a function of turbulence intensity for different grids, flow velocities and grid distances; lines represent formulas (23), (24) and (25).

5.6 Correlations of the Transition

The freestream turbulence intensity at the leading edge for grids G1 – G4 was from $Tu = 0.4$ % to 3.4 % and for grid G5 exceeded the value of 4 %, moreover the turbulence was not isotropic at the measured points in case of grid G5. Fig. 13 shows dependence between the turbulence intensity at the plate leading edge, Tu, and the momentum thickness Reynolds number of the onset of transition, Re_t^{**}, in comparison with some known correlations: Hourmouziadis (1989):

$$\mathrm{Re}_t^{**} = 460 Tu^{-0.65} \tag{23}$$

Mayle (1991):

$$\mathrm{Re}_t^{**} = 400 Tu^{-5/8} \tag{24}$$

And Abu-Ghannam and Shaw (1980):

$$\mathrm{Re}_t^{**} = 163 + \exp(6.91 - Tu) \tag{25}$$

One can see, that for $Tu < 2$ % (it refers to grids G1, G2 and partly G3) the transition inception appears earlier than it follows from the mentioned correlations.

To create the first correlation with turbulence length scale, the dissipation scale Lu values at the leading edge of the plate were used. The results of present investigations seem to confirm the results of Jonas (2000), but only if we make correlation for all grids together (Fig. 14a; dashed line represents the Eq. (1)). But when we look at every grid separately, the result seems not to be that obvious. Because of the result points dispersion the investigations need to be verified, but according to the present ones the momentum thickness Reynolds number Re_t^{**} increases (which means the transition appears later) when Lu increases, for grids G2 and G3. If the values of the Reynolds number Re_t^{**} start to become smaller than 200 (as we have for the grid G5), the transition appears earlier when the values of the length scale Lu are larger.

The turbulence scale at the Eq. (1) can be changed in the non – dimensional formula using one of the grid parameters. Wire diameter, d, has been chosen:

$$\mathrm{Re}_t^{**} = k\left(\frac{Lu}{d}\right)^m \tag{26}$$

Figure 14b shows the results for Re_t^{**} as a function of Lu/d, for grids of different dimensions. For G1 – G4: coefficient of the Eq. (26) is $k = 158$, exponent $m = 0.455$. When the value of Lu/d increases, the transition appears later for the grids G1 – G4 and earlier for the grid G5, but we keep in mind that in the last case the turbulence is anisotropic. Besides, the values for the grid G4 seem to belong to both correlations. It is interesting to note that the minimum value of transition Reynolds number presented in Figs. 14a and 14b is in a good agreement with the classical solution obtained from the theory of hydrodynamic stability: $Re_t^{**} = 161$.

Because in case of the grid G5 turbulence was neither isotropic nor homogeneous at the measured points over the plate, it seems reasonable to neglect the results for this grid in the following part of the article.

The next correlations, presented below, refer to free stream turbulence intensity, Tu_t, and free stream turbulence dissipation length scale, Lu_t, at the onset of transition. (Having determined the point of the beginning of transition and profiles of intensity and scale behind grids, values of Tu_t and Lu_t were found). Fig. 15 presents Re_t^{**} as a function of Tu_t. Again, for grids G1, G2, where $Tu_t < 1$%, we can't

find any good correlation function for Tu_t and Re_t. The next Fig. 16 displays Re_t^{**} as a function of the dissipation length scale Lu_t at the onset of transition. For small levels of free stream turbulence, i.e. Tu_t< 1.5 % (which was obtained for grids G1, G2 and almost for all used velocities and grid distance L_s in case of G3 (U = 6, 10 m/s for all grid distances and U = 15 m/s for L_s = 450, 410, 370 mm), the dissipation scale increases with the decreasing of Re_t^{**}. For the further increasing of the level of turbulence, i.e. for G3 (U = 15 m/s, L_s = 330 mm and U = 20 m/s, L_s = 370, 330 mm) and for G4 (U = 6 and 10 m/s, all grid distances) the influence of the turbulence scale on the beginning of transition isn't significant. Fig. 17 displays the relation between turbulence scale and intensity at the onset of transition. With the increasing of Tu_t, Lu_t also increases, but only to the level of turbulence $Tu_t \approx$ 1.5 %, then Lu_t slowly starts to reach a constant value.

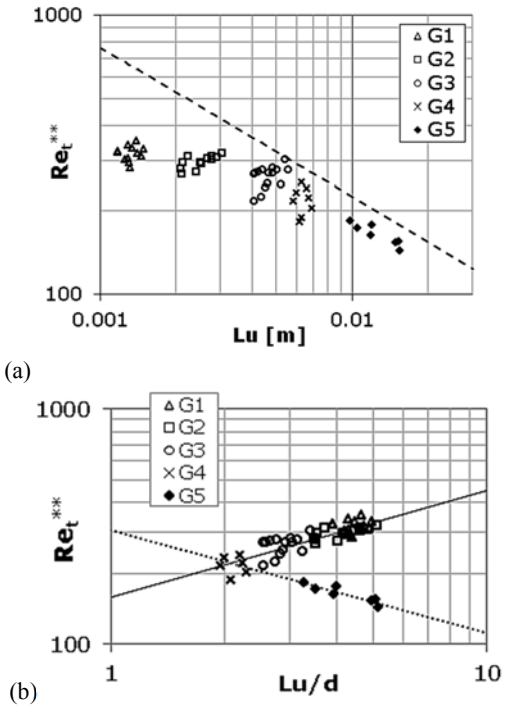

Fig. 14. Momentum thickness Reynolds number at the onset of transition as a function of *Lu*, (Fig.14a) and *Lu /d* (Fig.14b) for different grids, flow velocities and grid distances; dashed line in Fig.14a represents the Eq. (1).

The correlation $Re_t^{**} = f(Lu_t)$ can be made non – dimensional by means of the momentum thickness of the boundary layer, δ^{**}:

$$\mathrm{Re}_t^{**} = k\left(Lu_t / \delta_t^{**}\right)^m \tag{27}$$

Figure 18 presents Re_t^{**} as a function of Lu_t divided by the momentum thickness at the onset of transition, δ_t^{**} (δ_t^{**} was found from the formula $Re_t^{**} = U\,\delta_t^{**}/\nu$, where U – streamwise velocity, ν – kinematic viscosity). One can observe a similar trend as for previous correlation (Fig. 16). For small levels of turbulence, Tu_t< 1.5 % (G1, G2, G3), dissipation scale divided by δ_t^{**} increases with slight decreasing of Re_t^{**}. For Tu_t> 1.5 % (G4 and G3: U = 15 m/s, L_s = 330 mm and U = 20 m/s, L_s = 370, 330 mm) further decreasing of Re_t^{**}seems not to depend on changes in the ratio $Lu_t/\,\delta_t^{**}$, which tends to the constant value.

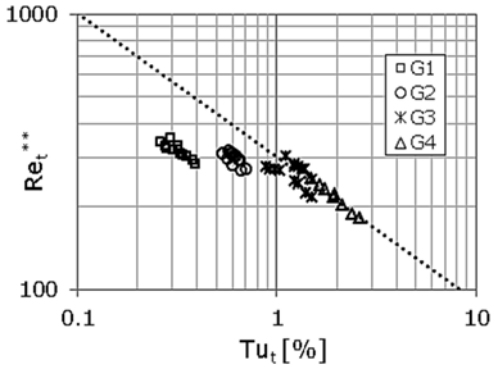

Fig. 15. Momentum thickness Reynolds number at the onset of transition as a function of turbulence intensity Tu_t, at the onset of transition, for different grids, mean flow velocities and grid distances.

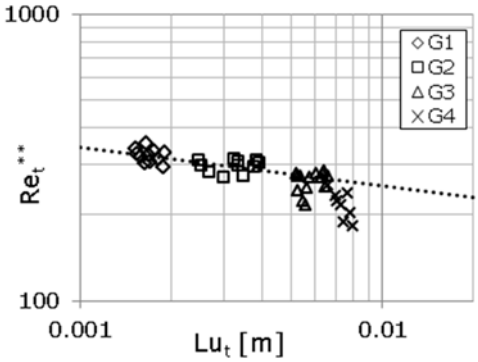

Fig. 16. Momentum thickness Reynolds number as a function of turbulence scale Lu_t, at the onset of transition, for different grids, mean flow velocities and grid distances.

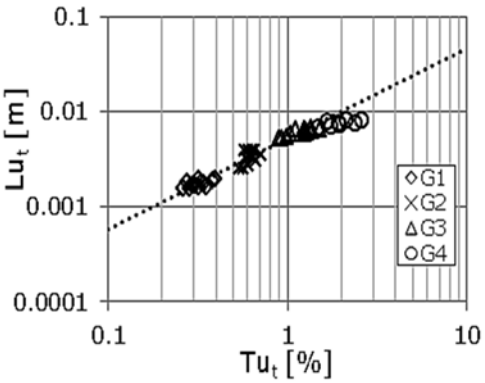

Fig. 17. Dissipation length scale Lu_t as a function of turbulence intensity Tu_t, at the onset of transition, for different grids, mean flow velocities and grid distances.

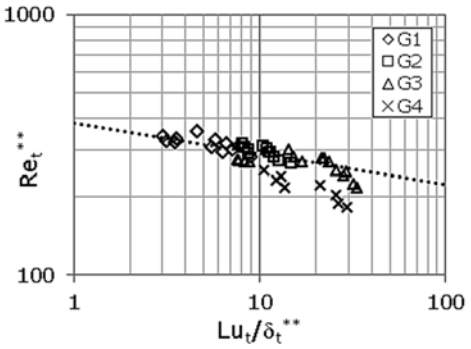

Fig. 18. Momentum thickness Reynolds number as a function of the ratio Lu_t/δ_t^{**} at the onset of transition, for different grids, mean flow velocities and grid distances.

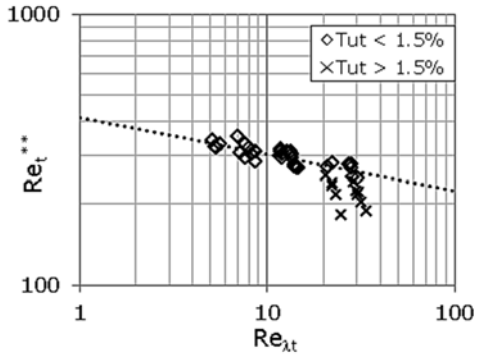

Fig. 19. Momentum thickness Reynolds number as a function of the Taylor Reynolds number at the onset of transition, for different grids, mean flow velocities and grid distances.

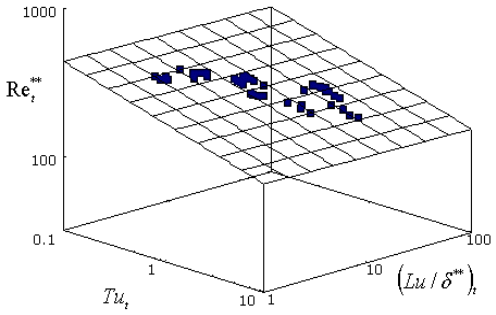

Fig. 20. Momentum thickness Reynolds number as a function of turbulence intensity, Tu_t, and ratio Lu_t/δ_t^{**} at the onset of transition.

The next correlation is related with another turbulence length scale: Taylor microscale λ. The information about λ is sufficient to parameterize by-pass transition with free-stream turbulence intensity and scale, since it leads over dissipation rate $\varepsilon = 15\nu u'^2/\lambda^2$ (where u' is the streamwise velocity standard deviation) and turbulent kinetic energy to other scales and permits to link, over the transport equations, with the turbulent stresses. Fig.19 displays the onset Reynolds number Re_t^{**} as a function of Taylor Reynolds number $\mathrm{Re}_{\lambda t} = \dfrac{u'\lambda}{\nu}$ at the onset of transition. This time all data presented in Fig. 19 (for grids G1 – G4) are divided into two ranges: for $Tu_t \in (0.26;1.5)\%$ and, $Tu_t \in (1.5;2.6)\%$ which correspond to values of the turbulence level at the leading edge: $Tu_t \in (0.4;2)\%$, $Tu_t \in (2;3.4)\%$, respectively. As previous, the first range concerns with grids G1, G2 and G3 (U = 6, 10 m/s for all grid distances and U = 15 for L_s= 450, 410, 370 mm), the second range concerns with grid G3 (U = 15 m/s, L_s = 330 mm and U = 20 m/s, L_s = 370, 330 mm) and G4 (U = 6 and 10 m/s, all grid distances). When Tu_t < 1.5 % the onset of transition approaches the plate leading edge with the increasing of $\mathrm{Re}_{\lambda t}$. After exceeding the level of 1.5%, the onset Taylor Reynolds number starts to tend to the constant value.

Finally, two last Figs. (20, 21) present simultaneous impact of turbulence intensity and turbulence scale on the boundary layer transition. Taking into account the turbulence intensity, Tu_t, at the onset of transition and the turbulence scale, Lu_t, divided by the momentum thickness at the onset of transition, δ_t^{**}, we can write the Eq. (28), which is – to some extent – generalization of the correlation given by the Eq. (27).

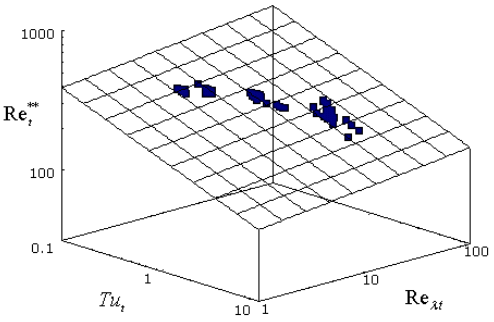

Fig. 21. Momentum thickness Reynolds number as a function of turbulence intensity, Tu_t, and Taylor Reynolds number, $\mathrm{Re}_{\lambda t}$, at the onset of transition.

$$\mathrm{Re}_t^{**} = kTu_t^{m_1}\left(\frac{Lu_t}{\delta_t^{**}}\right)^{m_2} \tag{28}$$

Taking logarithm of the above formula, we get an equation of a plane:

$$\log \mathrm{Re}_t^{**} = \log k + m_1 \log Tu_t + m_2 \log\left(\frac{Lu_t}{\delta_t^{**}}\right) \tag{29}$$

which is displayed in Fig. 20.The searched constants at the above formula were found by means of the three-dimensional regression procedure: k = 271, m_1 = – 0.206, m_2 = – 0.015. Analogously, a correlation related to the Taylor Reynolds number at the onset of transition can be written:

$$\mathrm{Re}_t^{**} = kTu_t^{m_1}\,\mathrm{Re}_{\lambda t}^{m_2} \tag{30}$$

The Eq. (30) is displayed in Fig. 21 and the searched constants are: $k = 201$, $m_1 = -0.287$, $m_2 = 0.088$. Looking at above two formulas (28), (29) and the exponentsm_1, m_2 it can be stated that turbulence intensity is the primary factor affecting transition while turbulence length scale has only a secondary affect.

6. CONCLUSION

To investigate the phenomena of turbulent flow, five wicker grids with square meshes and different parameters were used to generate turbulence. The turbulence intensity at the leading edge of the plate was from Tu = 0.4 % to 4 %. Several longitudinal scales of turbulence were determined, i.e. integral scale L, dissipation scale Lu, Taylor microscale λ and Kolmogorov scale η. To assess the isotropy of turbulence, the skewness factor of the flow velocity distribution was determined. For grids G1 to G4, i.e. for (d = 0.3 mm, M = 1 mm, Tu = 0.4 %) to (d = 3 mm, M = 10 mm, Tu = 3.4 %) the isotropic homogeneous turbulence throughout the measured chamber was obtained.

The influence of the turbulence scale on the laminar–turbulent bypass transition location on a flat plate was investigated. In this case the dissipation scale Lu at the leading edge was taken into account. For this purpose, the momentum thickness Reynolds number Re_t^{**}, at which transition onset appears, was calculated. Present investigations seem to confirm the results indicating that the boundary layer laminar–turbulent inception moves downstream with the decreasing of turbulence scale, but only if we make correlation for all grids together. When we take into account a single grid, especially G2 (d = 0.6 mm, M = 3 mm) and G3 (d = 1.6 mm, M = 4 mm), the results are not so obvious or even seem to be quite opposite.

Dividing the turbulence scale by the grid wire diameter, non–dimensional formula was developed (26). The investigation indicates that the reducing of turbulence scale (divided by the grid wire diameter d) provides an earlier inception, i.e. the lower momentum thickness Reynolds number for grids G1 – G4.

The next presented correlations, refer to free stream turbulence intensity, Tu_t, and free stream turbulence dissipation length scale, Lu_t, at the onset of transition. It was observed that for small levels of free stream turbulence (Tu_t< 1.5 %) the dissipation scale Lu_t increases with the decreasing of Re_t^{**}. For Tu_t> 1.5 %, the influence of the turbulence scale on the beginning of transition isn't significant. Similar conclusion was obtained for Lu_t divided by the momentum thickness at the onset of transition, δ_t^{**} (27). For Tu_t< 1.5 % the ratio Lu_t/δ_t^{**} increases with slight decreasing of Re_t^{**}; for higher level of turbulence, Lu_t/δ_t^{**} tends to the constant value. The onset Reynolds number Re_t^{**} as a function of Taylor Reynolds number $Re_\lambda = u'\lambda/\nu$ (where λ is Taylor microscale) at the onset of transition was presented. It was observed that for the intensity range $Tu_t \in (0.26;1.5)\%$, which corresponds to values of the turbulence level at the leading edge, $Tu \in (0.4;2)\%$, the onset of transition approaches the plate leading edge with the increasing of $Re_{\lambda t}$. For $Tu_t \in (1.5;2.6)\%$ $Tu \in (2;3.4)\%$ at the leading edge) the onset Taylor Reynolds number starts to tend to the constant value.

Finally, simultaneous impact of turbulence intensity and turbulence scale at the onset of transition on the boundary layer transition inception was presented (Figs. 20, 21), showing that turbulence intensity is the primary factor affecting transition and turbulence length scale has a secondary affect.

REFERENCES

Abu-Ghannam, B. J. and R. Shaw (1980).Natural transition of boundary layers – the effects of turbulence, pressuer gradient, and flow history. *J. Mech. Eng. Sci*. 22, 213-228.

Ames, F. E. and R. J. Moffat (1990). Heat transfer with high intensity, large scale turbulence: the flat plate turbulent boundary layer and the cylindrical stagnation point. *Report No. HMT-44,* Department of Mechanical Engineering, Stanford University, Stanford, CA.

Baines, W. D. and E. G. Peterson (1951). An investigation of flow through screens. *ASME J. Fluids Eng*.73, 467-480.

Barret, M. J. and D. K. Hollingsworth (2001). On the calculation of length scales for turbulent heat transfer correlation. *ASME J. Heat Transfer* 123, 878-883.

Batchelor, G. K. (1953).*The Theory of Homogeneous Turbulence*, Cambridge University Press, Cambridge, UK

Birouk, M., B. Sarh and I. Gokalp (2003). An attempt to realize experimental isotropic turbulence at low reynoldsnumber. *Flow Turbul. Combust.* 70, 325–348.

Blasius, P. R. H. (1913). Blasius, H. (1913). *The law of similarity of frictional processes in fluids*. (Originally in German), Forsch Arbeit Ingenieur-Wesen, Berlin 131. 1–41.

Dhawan, S. and R. Narasimha (1958). Some properties of boundary layer flow during the transition from laminar to turbulent motion. *J. Fluid Mech.* 3(04), 418-436.

Emmons, H. W. (1951). The laminar-turbulent transition in a boundary layer, Part I. *J. Aeron. Sci.* 18, 490-498.

Epik, E. J., E. P. Dyban, V. N. Klimenko, T. T. Suprun and L. E. Jushina (1998). *Experimental study of by-pass transition heat transfer,* Final report, Kiev.

Fouladi, F., P. Henshaw and D. S. K. Ting (2015). Turbulent Flow Over a Flat Plate Downstream of a Finite Height Perforated Plate. *ASME J. Fluid Eng*. 137, 021203-1.

Gad-el-Hak, M. and S. Corrsin (1973). Measurements of the nearly isotropic

turbulence behind a uniform jet grid.*J. Fluid Mech*. 62**,** 115-143.

Grzelak, J. and Z. Wiercinski (2015). The decay power law in turbulence generated by grids. *Transactions IFFM* 130, 93-107.

Hall, D. J. and J. C. Gibbings (1972). Influence of stream turbulence and pressure gradient on boundary – layer transition. *J. Mech. Eng. Sci*. 14, 134-146.

Hinze, I. O. (1975). *Turbulence*. McGraw – Hill Book Company.

Hourmouziadis, J. (1989). Aerodynamic Design of Low Pressure Turbines. AGARD *Lecture Series* 167.

Jimenez, J. (1998). Turbulent velocity fluctuations need to be Gaussian.*J. Fluid Mech*., 376, 139-147.

Johnson, M. W. and A. Pinarbasi (2014). The Effect of Pressure Gradient on Boundary Layer Receptivity. *Flow Turb. Combust*. 93, 1-24.

Jonas, P., O. Mazur and V. Uruba (2000). On the receptivity of the by – pass transition to the length scale of the outer stream turbulence. *Eur. J. Mech. B-Fluids*19, 707-722.

Kurian, T. and J. H. M. Fransson (2009). Grid-generated turbulence revisited. *Fluid Dynamics Research* 41(2).

Laws, E. M. and J. L. Livesey (1978). Flow through screens.*Ann. Rev. Fluid Mech.* 10,247-266.

Lipson, C. and N. J. Sheth (1973). *Statistical design and analysis of engineering experiments*. McGraw-Hill, New York.

Makita, H. (1991). Realization of a large-scale turbulence field in a small wind tunnel. *Fluid Dynamics Research* 8, 53-64.

Mayle, R. E. (1991). The Role of Laminar – Turbulent Transition in Gas Turbine Engines. *Journal of Turbomachinery* 113, 509-537.

Mohamed, M. S. and J. C. LaRue (1990). The decay power law in grid-generated turbulence. *J. Fluid Mech*. 219, 195-214.

Morkovin, M. V. (1969). On the many faces of transition, In *Viscous Drag Reduction*, ed. CS Wells, New York: Plenum, 1–31.

Mydlarski, L. and Z. Warhaft (1996). On the onset of high-Reynolds-number grid-generated wind tunnel turbulence.*J. Fluid. Mech*.320, 331-368.

Mydlarski, L. and Z. Warhaft (1998). Passive scalar statistics in high-Peclet-number grid turbulence.*J. Fluid. Mech*. 358,135-175.

Noro, S., Y. Suzuki, M. Shigeta, S. Izawa and Y. Fukunishi (2013).Boundary layer receptivity to localized disturbances infreestream caused by a vortex ring collision. *Journal of Applied Fluid Mechanics* 6 (3), 425-433.

Roach, P. E.(1986). The generation of nearly isotropic turbulence by means of grids.*J. Heat and Fluid Flow* 8 (2), 82–92.

Shahinfar, S. and J. H. M. Fransson (2011). Effect of free-stream turbulence characteristics on boundary layer transition.*J. Physics: Conference Series* 318(3).

Sreenivasan, K. R. (1982).Laminarescent, relaminarizing and retransitional flows.*Acta Mech.* 44**,** 1-48.

Ting, D. S. K. (2013*). Some Basics of Engineering Flow Turbulence*. Revised ed., Naomi Ting's Book, Windsor, Canada.

Townsend, A. A. (1948). Local isotropy in the turbulent wake of a circular cylinder.*Aust. J. Sci. Res.* 1(2), 161-174.

Valente, P. C. and J. C. Vassilicos (2011). The decay of turbulence generated by a class of multiscale grids. *J. Fluid Mech.* 687, 300-340.

Wadsworth, H. M. (1989). *Handbook of statistical methods for engineers and scientists*. McGraw-Hill, New York.

Wiercinski, Z. (1997). The stochastic theory of the natural laminar-turbulent transition in the boundary layer. *Trans. IFFM*, Gdansk102, 89-110.

Xu, J. K., J. Q. Bai, L.Qiao and Y. Zhang (2016). Correlation-Based Transition Transport Modeling for Simulating Crossflow Instabilities. *Journal of Applied Fluid Mechanics* 9(5), 2435-2442.